

## Supplemental Information

### Materials and Methods

#### *Reagents*

PL45 cells (Human pancreatic ductal adenocarcinoma cell line, SC0189) and DU145 cells (Human prostate cancer cell line, SC0128) used in this study were purchased from China Yuchi Cell (Shanghai) Biological Technology Co., Ltd. DMEM medium (KGM12800-500) containing 0.8 U/ml penicillin and 0.08 mg/ml streptomycin was purchased from KeyGEN Biotechnology (China). MEM medium (B210901) and penicillin-streptomycin (100X, B210801) was purchased from BasalMedia (China). Fetal bovine serum (FBS, JC63487) was purchased from CLARK Biosciences (China). 1X Phosphate Buffered Saline (PBS, 21144756) buffer was purchased from Biosharp Life Sciences (China). Bull Serum Albumin (BSA, No. H1130) was purchased from Solarbio (China). Monoclonal antibody of purified mouse antihuman CD71 for flow cytometry was purchased from BD Biosciences Pharmingen. Mouse monoclonal antibody integrin  $\beta$ 1(K-20):sc-18887 (anti $\beta$ 1(K-20)), integrin  $\alpha$ 3(P1B5) antibody:sc-13545 (anti $\alpha$ 3(P1B5)), and integrin  $\alpha$ 3(VM-2) antibody:sc-32237 (anti $\alpha$ 3(VM-2)) were purchased from SANTA CRUZ Biotechnology.

#### *Cell Culture*

PL45 cells were cultured in DMEM medium and DU145 cells were cultured in MEM medium at 37 °C atmosphere with 5 % CO<sub>2</sub>. In cell processing, the washing buffer contained 4.5 g/L glucose and 5 mM MgCl<sub>2</sub> in PBS buffer, and the binding buffer was prepared by adding 1 % BSA into the washing buffer to reduce background binding. The number of cells for final flow cytometric analysis was approximately  $3 \times 10^5$  as estimated by blood counting chamber.

#### *Synthesis of gold nanoparticle with a diameter of 5 nm (G<sub>5</sub>NP)*

G<sub>5</sub>NP were synthesized according to the method mentioned in previous study.<sup>1</sup> In brief, preparation of solution A: 1 mL of a 1 % by mass solution of HAuCl<sub>4</sub> was added to 79 mL of double-distilled water, and the solution was heated to 60 °C. Next, preparation of solution B: 4 mL of 1 % by mass solution of sodium citrate and 0.5 mL of 1 % Tannic acid were added into 20 mL of double-distilled water. Production of G<sub>5</sub>NP was initiated by addition of solution A into solution B and heating at 60°C for 5 min, and then the whole solution was cooled to room temperature in an ice box. The size and absorption spectra of G<sub>5</sub>NP were verified with a JEM-

2100F transmission electron microscope (TEM) and a UV-2600 UV-VIS spectrophotometer.

### ***Conjugation of G<sub>5</sub>NP and antibody (G<sub>5</sub>@antibody)***

The strategy for coupling G<sub>5</sub>@antibody conjugates followed the previously published procedure.<sup>2,3,4</sup> Briefly, different volume (0.2, 0.8, 1.0, 1.2, 1.5, and 2.0  $\mu$ L) of antibody CD71 (antiCD71) was added to 200  $\mu$ L of G<sub>5</sub>NP solution, followed by adjusting pH to 7.5. The mixed solution was then incubated at 37 °C, 200 rpm/min, for 3 h. After that, the mixed solution was centrifuged at 11000 rpm/min for about 30 min, followed by resuspension with 200  $\mu$ L PBS buffer containing 0.1 % BSA. Detection was performed under UV-2600 UV-VIS spectrophotometry. As the volume of antibody increased, more G<sub>5</sub>NP were conjugated with antibody with a corresponding increase in absorption, thus maximizing the number of G<sub>5</sub>@antibody, contributing still more antibody available to bind the corresponding receptor protein. The coupling process of antibody integrin  $\alpha$ 3 (anti $\alpha$ 3(P1B5)) and antibody integrin beta 1 (anti $\beta$ 1(K-20)) was similar to that of antiCD71, except for adjusting pH to 7.0, and the different volumes were 0.2, 0.4, 0.8, 1.0, 1.2, and 1.5  $\mu$ L, respectively. The imaging of G<sub>5</sub>@antibody was also determined using agarose gel electrophoresis, zeta potential, AFM and TEM with negative staining.

### ***TEM Analysis of Negative Staining and AFM Analysis***

To examine whether G<sub>5</sub>NP had been conjugated with antibody or not, TEM analysis of negative staining<sup>5,6</sup> and AFM<sup>7,8</sup> were applied in this paper. In short, 10  $\mu$ L of G<sub>5</sub>@antibody conjugates solution, 10  $\mu$ L of native antibody solution, and 10  $\mu$ L of native G<sub>5</sub>NP solution were allowed to absorb onto a copper grid (300 mesh) for about 10 min, respectively. The additional liquid was then removed by suction with rough edges of filter paper. Next, the grids were covered in 10  $\mu$ L volume of 2 % (w/v) phosphor tungstic acid (PTA) of pH 7.0  $\pm$  0.2 for 1 min. The redundant liquid was removed with rough edges of filter paper, as well. Last, images of the grids were observed under the Jeol JEM 1230 electron microscope operated at 80 kV. It should be noted that AFM analysis was carried out in a manner similar to the procedure of TEM analysis, except the copper grid (300 mesh) was replaced with mica flakes with no staining PTA staining. AFM images were observed on a Dimension Icon Microscope (Bruker, America) and analyzed with Nano scope v7.3 software.

### ***Confocal Imaging Analysis***

The integrity of cell nucleus was examined by staining the cells with DAPI dyes and observing under a Zeiss laser confocal microscope (LSM800) at 600V. First, about  $3 \times 10^5$  cells in a round culture plate with a diameter of 10 cm were digested by pancreatic enzymes and then suspended in 1 mL corresponding medium. Then, 150  $\mu$ L of cell suspension were added into a 24-well culture plate which included TC treatment thin glass for cell climbing slice. After overnight culture, the cells on the slide were fixed with 4 % paraformaldehyde for 30 min. Next, after washing 3 times with wash buffer, cells were blocked with 1 % skim milk for 30min and then washed again 3 times with wash buffer. Next, 20  $\mu$ L of DAPI solution previously diluted 500 times in PBS buffer were added to cover the thin glass for 10 min, followed by washing 3 times with wash buffer. Finally, cells were observed under confocal microscopy. The excitation source for the DAPI dyes was 405 nm.

NSET efficiency between aptamer and different  $G_5@$ antibody conjugates was observed under the confocal microscope (TCS SP 8) at 850 V. First, about  $3 \times 10^5$  cells in a round culture plate with a diameter of 10 cm were digested by pancreatic enzymes and then suspended in 1 mL corresponding medium. Then, 150  $\mu$ L of cell suspension were added into a 24-well culture plate, which included TC treatment thin glass for cell climbing slice, and cultured overnight. Next, after washing 3 times with PBS buffer, corresponding saturated concentrated aptamer-FAM (PL45 cells: 150 nM XQ-2d-FAM, DU145 cells: 100 nM DML7-FAM) and 80  $\mu$ M endocytosis inhibitor were added and co-incubated for corresponding time (PL45 cells: 30 min, DU145 cells: 60 min). Afterwards, cells were washed once and excess 600  $\mu$ L  $G_5@$ antibody were added for 3 h co-incubation. After further washing 3 times with wash buffer, cells were mounted with anti-fluorescence quenching agent. Finally, cells were observed under the confocal microscope. The excitation source for the FAM and DAPI dyes was 488 and 405 nm, respectively.

### ***Time-correlated single photon counting measurement on lifetime (FLT)***

To evaluate the quenching efficiency and FLT of FAM-labeled aptamer incubated with  $G_5@$ antibody on PL45 cells, Ultrafast Time Resolved Fluorescence Spectrometer was implemented. First, saturation concentration of FAM-labeled aptamer was incubated with cells ( $3 \times 10^5$ ) at 4 °C that could prevent receptor protein internalization with 80 rpm /min for the 30 min. After incubation, the cells were centrifuged at 4 °C and 900 rpm/min for 5 min, washed

by 600  $\mu\text{L}$  of washing buffer, and suspended in the 200  $\mu\text{L}$  DMEM medium. Next, 600  $\mu\text{L}$  volume of  $\text{G}_5\text{@antibody}$  solution was added to the cell suspension, and the whole system volume of 800  $\mu\text{L}$  was incubated at 4  $^\circ\text{C}$  at 80 rpm/min for another 3 hours. After that, cells were washed by 600  $\mu\text{L}$  volume of washing buffer. Finally, after centrifuged, the precipitates of cells were suspended in 200  $\mu\text{L}$  of binding buffer and subjected to detect by Ultrafast Time Resolved Fluorescence Spectrometer within 30 min at an appropriate temperature.

#### ***Flow Cytometric Analysis for Determination of Saturation Concentration***

Saturation concentration of FAM-labeled aptamer incubation with PL45 or DU145 cells was explored by determining the fluorescent intensity (FLI) of these cells, using flow cytometry at various concentrations. Briefly,  $3 \times 10^5$  cells were incubated with different concentration of aptamer-FAM at 4  $^\circ\text{C}$  for corresponding time. After incubation, cells were washed with 600  $\mu\text{L}$  of washing buffer and centrifuged at 4  $^\circ\text{C}$  and 900 rpm/min for 5 min, followed by repeating this step three times. After centrifugation, the cell precipitates were suspended in 200  $\mu\text{L}$  volume of binding buffer and subjected to flow cytometry within 10 min at an appropriate temperature. The FLI of these cells was detected under the BD Accuri™ C6 by calculating 10000 events.

#### ***Flow Cytometric Analysis for Verifying the Incubation Time***

To prepare FAM-labeled aptamer for monitoring the FLI of cells by flow cytometry incubation with PL45 or DU145, cells ( $3 \times 10^5$ ) were incubated with saturated concentrated aptamer-FAM (PL45 cells: 150nM XQ-2d-FAM; DU145 cells: 100nM DML7-FAM) at 4  $^\circ\text{C}$  for different time. Next, cells were washed with 600  $\mu\text{L}$  volume of washing buffer 3 times and centrifuged at 4  $^\circ\text{C}$  and 900 rpm/min for 5 min. After centrifugation, cell precipitates were suspended in 200  $\mu\text{L}$  volume of binding buffer and subjected to flow cytometry within 10 min at an appropriate temperature. The FLI of these cells was then determined using the BD Accuri™ C6 by counting 10000 events.

#### ***Flow Cytometric Analysis to Examine Quenching Efficiency***

To evaluate the quenching efficiency of FAM-labeled aptamer incubated with  $\text{G}_5\text{@antibody}$  on PL45 or DU145 cells, flow cytometry was implemented. First, saturation concentration of FAM-labeled aptamer was incubated with cells ( $3 \times 10^5$ ) at 4  $^\circ\text{C}$  using a table concentrator at 80 rpm/min to prevent receptor protein internalization for the corresponding

time (PL45 cells: 30 min; DU145 cells: 60 min). After incubation, the cells were washed with 600  $\mu$ L of washing buffer, centrifuged at 4 °C and 900 rpm/min for 5 min and suspended in the corresponding medium. Next, different volume of G<sub>5</sub>@antibody solution was added to the cell suspension, and the whole system volume of 800  $\mu$ L was incubated at 4 °C at 80 rpm for another 3 hours. After that, cells were washed with 600  $\mu$ L volume of washing buffer three times. Finally, the precipitates of cells were suspended in 200  $\mu$ L of binding buffer and subjected to flow cytometry within 10 min at an appropriate temperature. The FLI of these cells was detected using the BD Accuri™ C6 by counting 10000 events.

### ***Flow Cytometric Analysis for Detection of Competitive Binding***

We assessed competitive binding between FAM-labeled aptamer and native antibody on receptor protein on the surface of PL45 or DU145 cell membrane protein by detecting the FL of various cell samples. Cells ( $3 \times 10^5$ ) were incubated with native FAM-labeled aptamer at 4 °C for 30 min (XQ-2d-FAM) or 60 min (DML7-FAM). Cells were then washed with 600  $\mu$ L volume of washing buffer, centrifuged at 4 °C and 900 rpm/min for 5 min and suspended in the corresponding medium. Next, different volume of native antibody solution was added to the cell suspension, and the whole system was incubated at 4 °C at 80 rpm/min for another 3 hours. Next, cells were washed with 600  $\mu$ L volume of washing buffer three times. Eventually, cell precipitates were suspended in 200  $\mu$ L volume of binding buffer and subjected to flow cytometry within 10 min at an appropriate temperature. The FLI of these cells was detected using the BD Accuri™ C6 by counting 10000 events.

## Supplemental figures

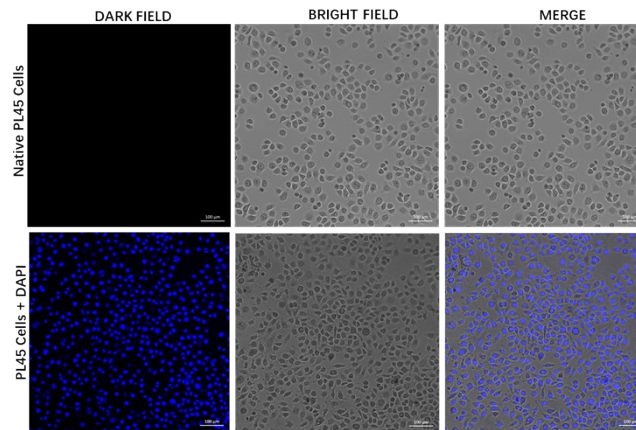


**Figure S1. Confocal imaging to monitor the integrity of PL45 cell nucleus.** DAPI-labeled PL45 cells (Left); native PL45 cells (Median) and the merge graph (Right) were observed by confocal microscopy. Scale bar is 100  $\mu\text{m}$ .

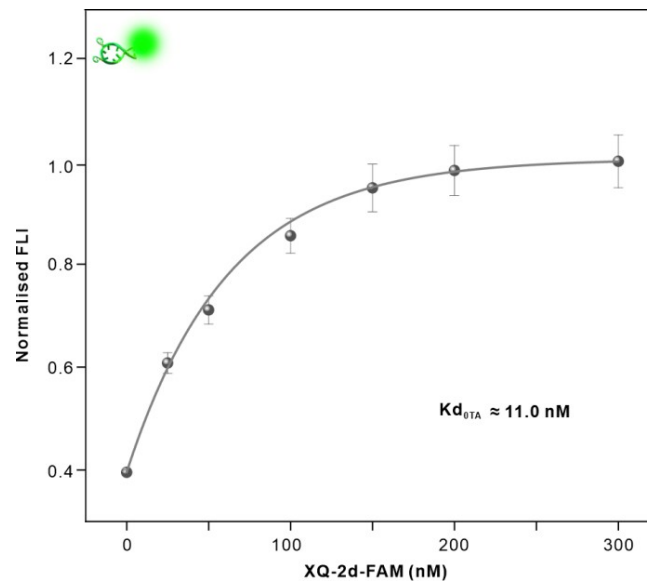


**Figure S2. The binding affinity to PL45 cells of XQ-2d-FAM.** PL45 cells incubated with different concentration of XQ-2d-FAM, i.e. i.e. 0, 25, 50, 100, 150, 200, and 300 nM, respectively.

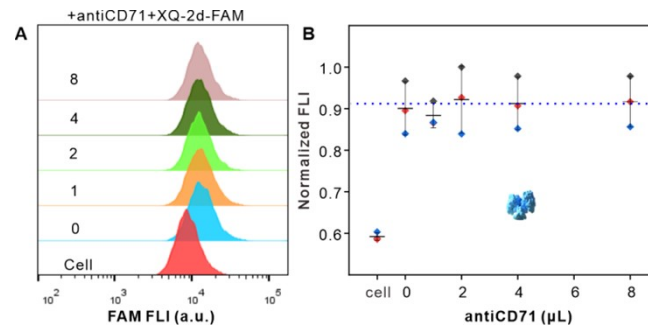


**Figure S3. Competitive binding assays by flow cytometry (FCM).** (A, B) Competitive binding assays on PL45 cells incubated with saturated XQ-2d-FAM and different amounts of antiCD71 including 1, 2, 4, and 8  $\mu\text{L}$ , respectively. And the order incubated with cells is antiCD71, XQ-2d-FAM.

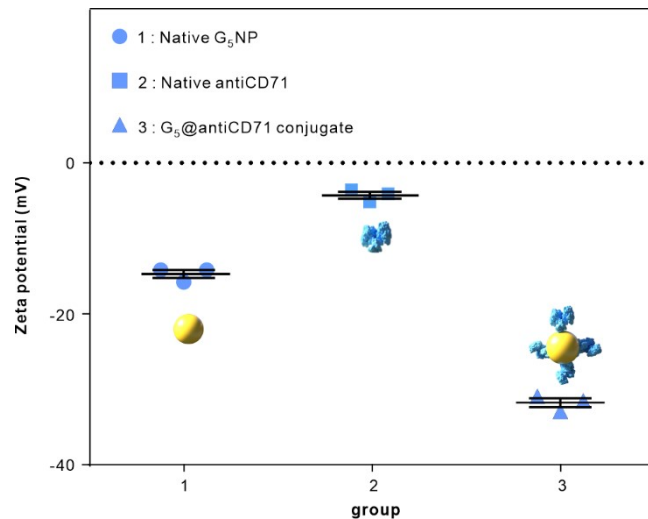


**Figure S4. Zeta potential assays of native  $G_5\text{NP}$ , native antiCD71, and  $G_5@$ antiCD71.** Zeta potential measurement of native  $G_5\text{NP}$  (group 1), native antiCD71 (group 2), and  $G_5@$ antiCD71 conjugates (group 3) by Zetasizer Nano-ZSE.

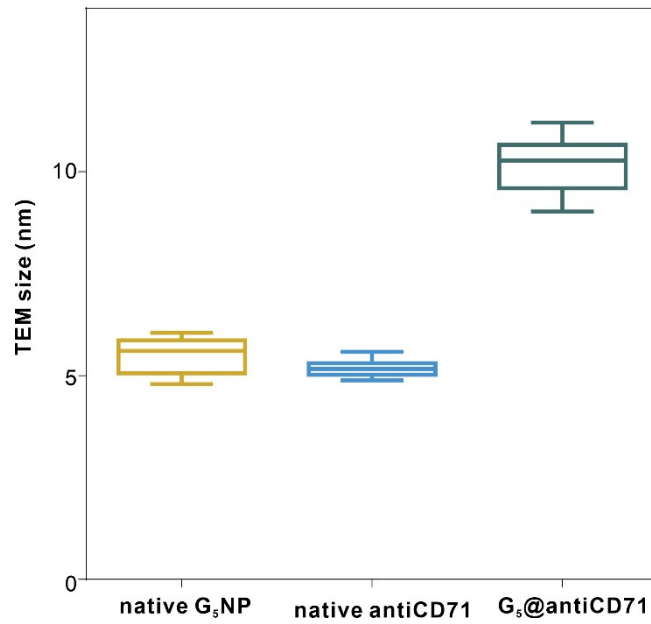


**Figure S5.** TEM size estimation of native G<sub>5</sub>NP, native antiCD71, and G<sub>5</sub>@antiCD71 in Figure 2E-G by ImageJ software, respectively.

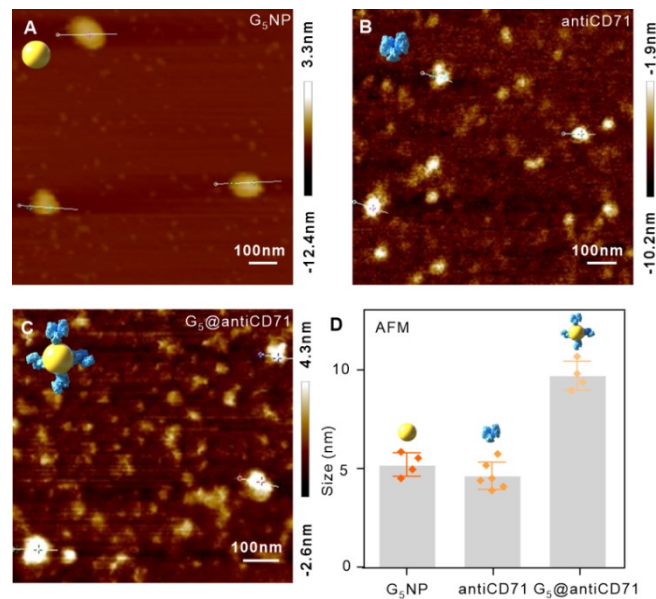


**Figure S6.** AFM assays of G<sub>5</sub>NP, native antiCD71, and G<sub>5</sub>@antiCD71. (A-C) AFM images of native G<sub>5</sub>NP, native antiCD71, and G<sub>5</sub>@antiCD71, respectively. (D) AFM size analysis of native G<sub>5</sub>NP, native antiCD71, and G<sub>5</sub>@antiCD71 by Nano Scope Analysis software.



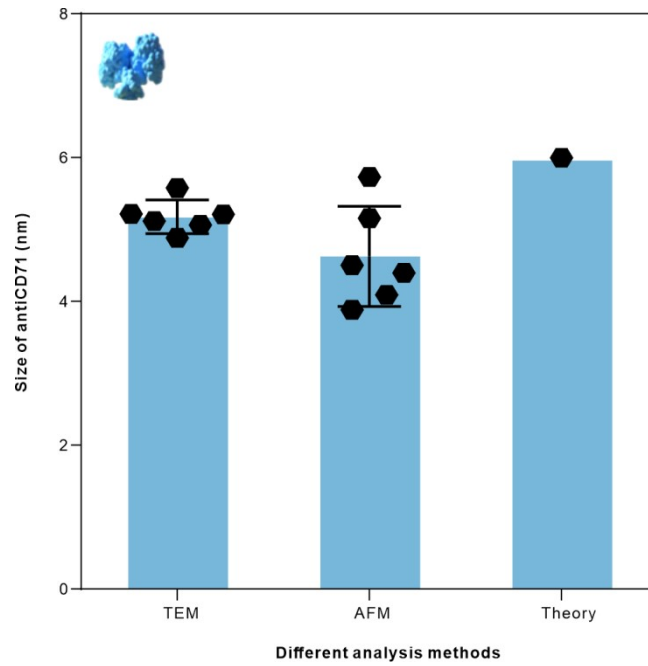


**Figure S7. Statistical analysis showed no significant differences in the sizes of antiCD71.** Size of antiCD71 antibody by three different methods, i.e., TEM, AFM, and theoretical calculation, respectively.

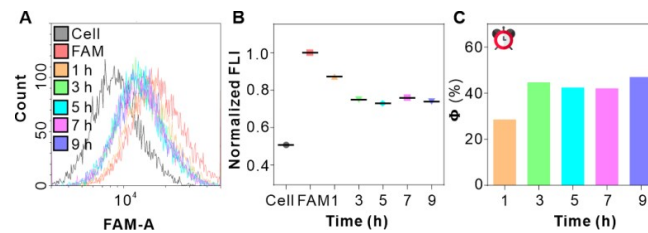


**Figure S8. FCM analysis on the best incubation time of G<sub>5</sub>@antiCD71 coupling with PL45 cells.** (A) Flow histogram of native PL45 cells (Cell), cells incubated with saturated XQ-2d-FAM (FAM), and cells with saturated XQ-2d-FAM then excess saturated G<sub>5</sub>@antiCD71 conjugates for different time i.e., 1, 3, 5, 7, 9 h, respectively. (B) Normalized FLI of these PL45 cells in A. (C) The corresponding fluorescence quenching efficiency ( $\Phi$ ) analysis of these cells in A.

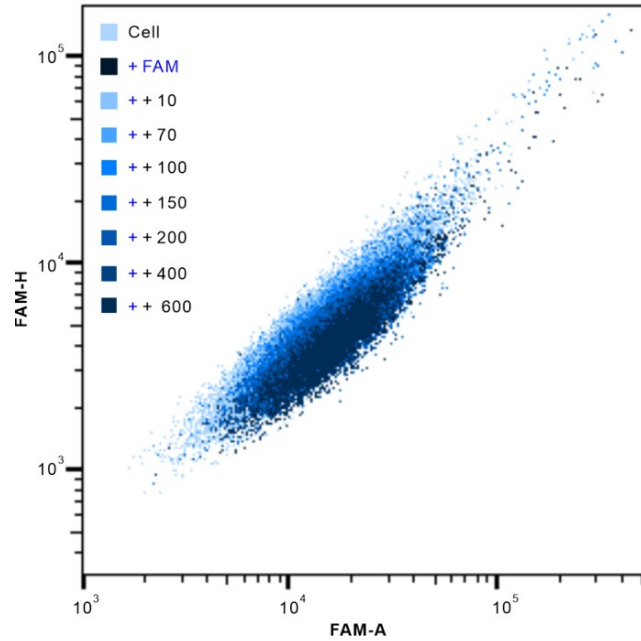


**Figure S9. The population and monodisperses of the PL45 cells.** From bottom to up are native PL45 cells (Cell); cells with saturated XQ-2d-FAM (+ FAM); cells with saturated XQ-2d-FAM and G<sub>5</sub>@antiCD71 of different amounts, i.e. 10, 70, 100, 150, 200, 400, and 600  $\mu$ L, respectively (from “+ + 10” to “+ + 600”).

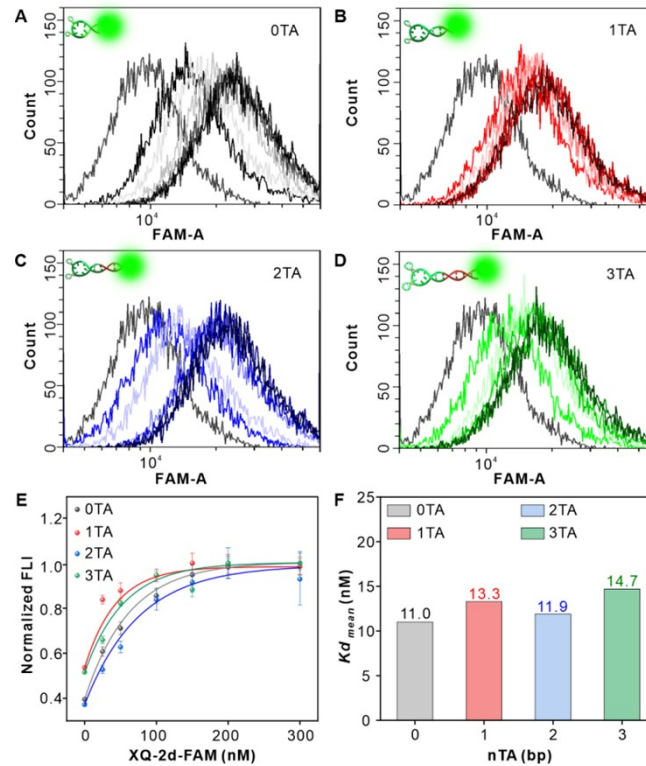


**Figure S10. The binding affinity to PL45 cells of XQ-2d-nTA-FAM.** (A-D) Flow histogram of PL45 cells incubated with different concentration of XQ-2d-nTA-FAM, i.e., 0, 25, 50, 100,

150, 200, and 300 nM, respectively. (E) Normalized FLI of these PL45 cells in A-D. (F) The equilibrium dissociation constants ( $K_d$ ) of XQ-2d-nTA-FAM to PL45 cells. “n” could be 0, 1, 2 and 3.

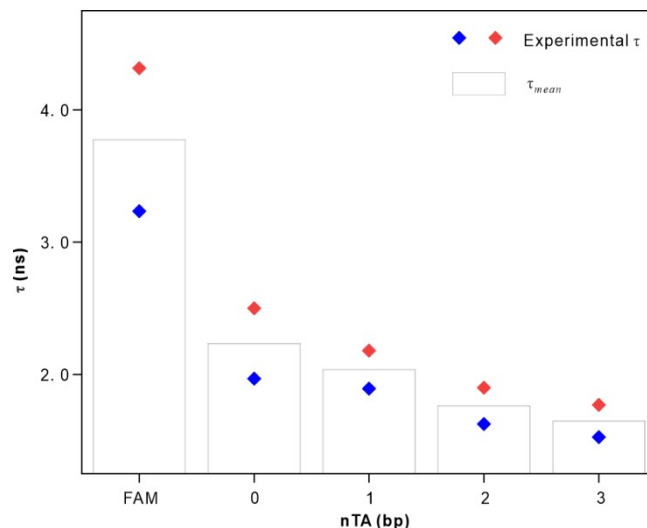


**Figure S11. Fluorescence lifetime of cells incubated with XQ-2d-FAM and cells incubated with XQ-2d-nTA-FAM then co-incubated with  $G_5@antiCD71$ . “n” could be 0, 1, 2 and 3.**

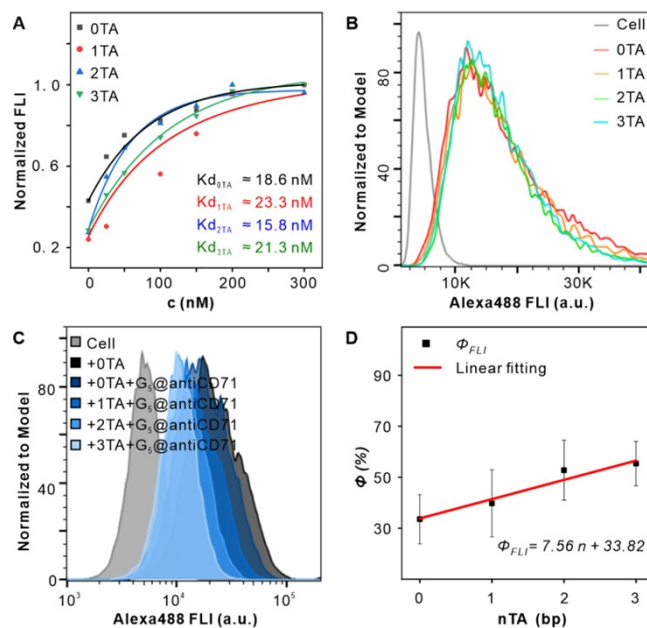


**Figure S12. SN-Nanoruler with a single-nucleobase resolution identified by using of Alexa488-GNP pair.** (A) The binding affinity to PL45 cells of XQ-2d-nTA-Alexa488. (B) FCM analysis of native PL45 cells (Cell), cells incubated with saturated XQ-2d-Alexa488 (0 TA), XQ-2d-1TA-Alexa488 (1 TA), XQ-2d-2TA-Alexa488 (2 TA), and XQ-2d-3TA-Alexa488 (3 TA), respectively. (C) FCM analysis of cell, cell with saturated 0TA, and cell with saturated 0, 1, 2, and 3 TA, then saturated  $G_5@antiCD71$ , respectively. Lengthening the “n

TA” spacer between the 5’ end of XQ-2d and Alexa488 dye, where n is the number of TA bases. (D) Relationship between the number of TA bases and  $\Phi$ , where  $\Phi$  was calculated according to change of Alexa488 FLI. “n” could be 0, 1, 2 and 3.

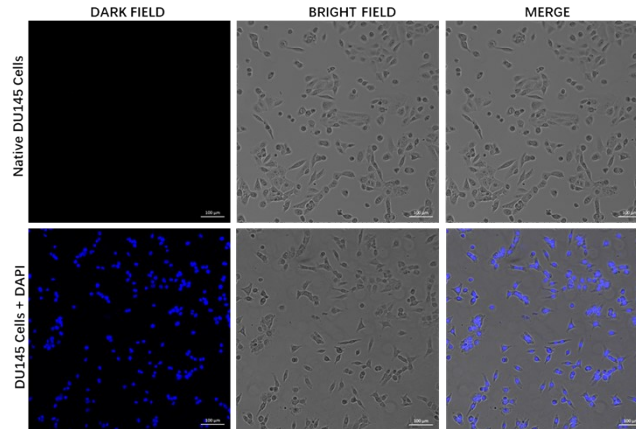


**Figure S13. Confocal imaging to monitor the integrity of DU145 cell nucleus.** DAPI-labeled DU145 cells (Left); native DU145 cells (Median) and the merge graph (Right) were visualized by confocal microscopy. Scale bar is 100  $\mu$ m. The nucleus was stained with DAPI.

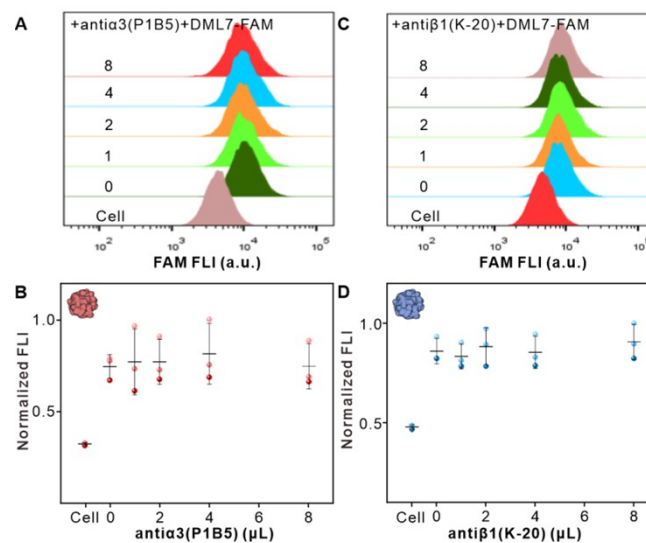


**Figure S14. Study of competitive binding between DML7-FAM aptamer and two antibodies: anti $\alpha$ 3(P1B5) and anti $\beta$ 1(K-20).** The order incubated with cells is antibody, DML7-FAM. (A, B) Competition detecting between DML7-FAM and different amounts of anti $\alpha$ 3(P1B5) antibody, i.e., 1, 2, 4, and 8  $\mu$ L, respectively. (C, D) Competition detecting between DML7-FAM and different amounts of anti $\beta$ 1(K-20) antibody, i.e., 1, 2, 4, and 8  $\mu$ L, respectively.

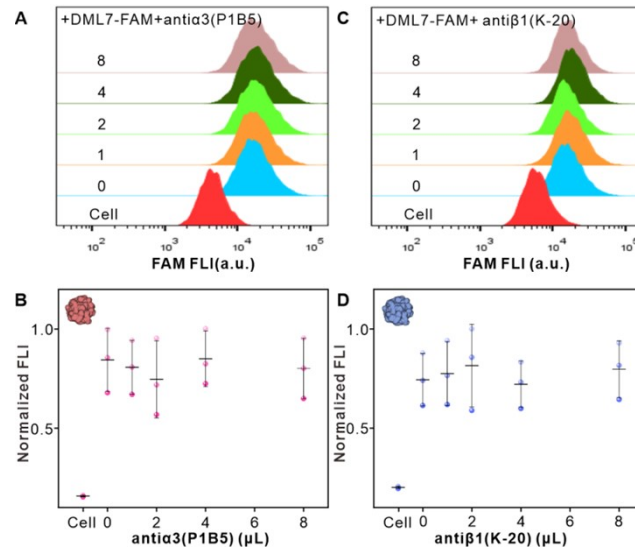


**Figure S15. Study of competitive binding between DML7-FAM aptamer and two antibodies: antiα3(P1B5) and antiβ1(K-20).** Antibody and aptamer were simultaneously incubated with cells. (A, B) Competitive binding assays on DU145 cells incubated with saturated DML7-FAM and different amounts of antiα3(P1B5) including 1, 2, 4, and 8 μL, respectively. (C, D) Competitive binding assays on DU145 cells incubated with saturated DML7-FAM and different amounts of antiβ1(K-20) including 1, 2, 4, and 8 μL, respectively.

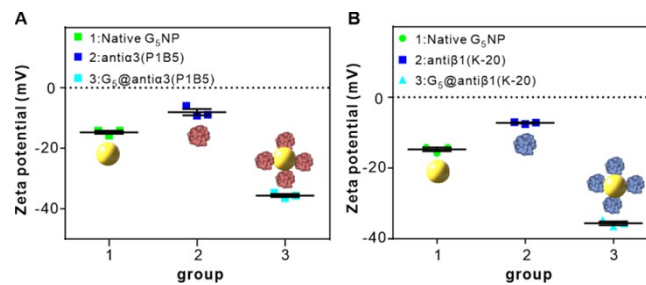


**Figure S16. Zeta potential assays of native G<sub>5</sub>NP, native antibody, and each G<sub>5</sub>@antibody.** (A, B) Zeta potential of native G<sub>5</sub>NP (group 1), native antibody (group 2), i.e., antiα3(P1B5) and antiβ1(K-20) and each G<sub>5</sub>@antibody (group 3), i.e., G<sub>5</sub>@antiα3(P1B5) and G<sub>5</sub>@antiβ1(K-20), respectively.

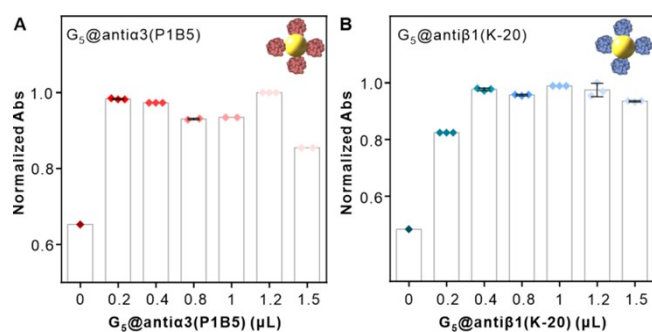


**Figure S17. UV-VIS absorbance spectroscopy assays of each  $G_5@antibody$ .** (A, B) Normalized absorbance of  $G_5@antibody$  conjugates for various volume of  $antia3(P1B5)$  (A) and  $anti\beta1(K-20)$  (B), i.e., 0, 0.2, 0.4, 0.8, 1.0, 1.2, and 1.5  $\mu\text{L}$ , respectively.

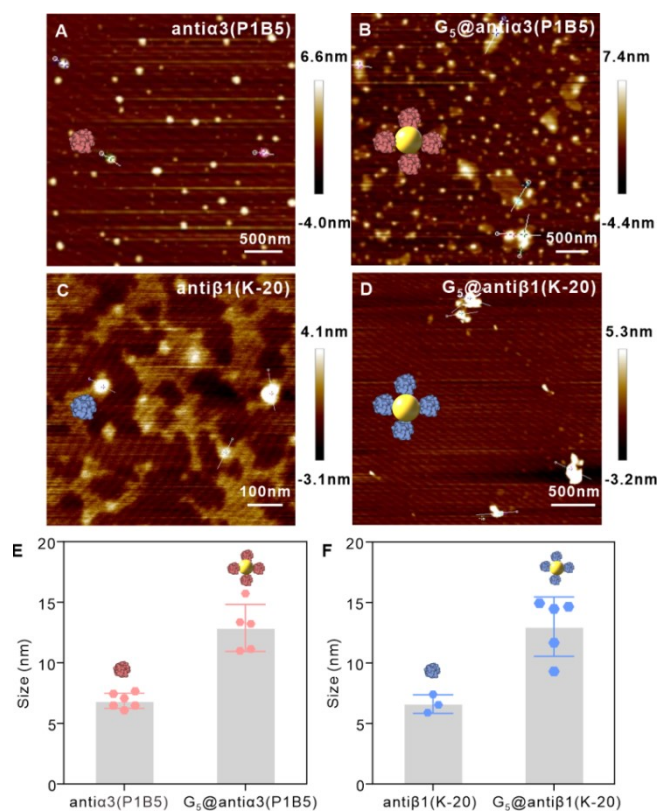


**Figure S18. AFM assays of  $G_5\text{NP}$ , native antibody, and  $G_5@antibody$ .** (A-E) AFM images of native  $antia3(P1B5)$ ,  $G_5@antia3(P1B5)$ ,  $anti\beta1(K-20)$ , and  $G_5@anti\beta1(K-20)$ , respectively. (E, F) AFM size analysis of native  $antia3(P1B5)$ ,  $G_5@antia3(P1B5)$ , native  $anti\beta1(K-20)$ , and  $G_5@anti\beta1(K-20)$  by Nano Scope Analysis software.

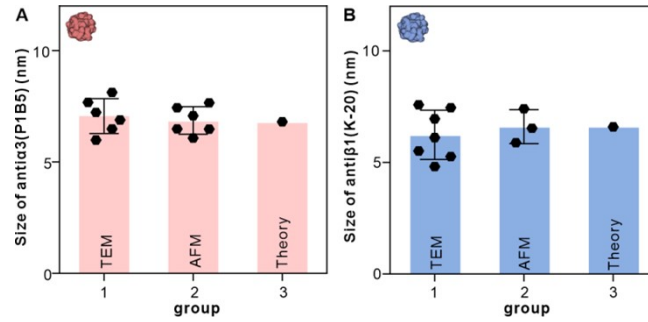


**Figure S19. Statistical analysis showed no significant differences in the sizes of each antibody.** (A, B) Size of native anti $\alpha$ 3(P1B5), and native anti $\beta$ 1(K-20) analysis by three methods, i.e., TEM (group 1), AFM (group 2) and the theoretical calculation (group 3), respectively.

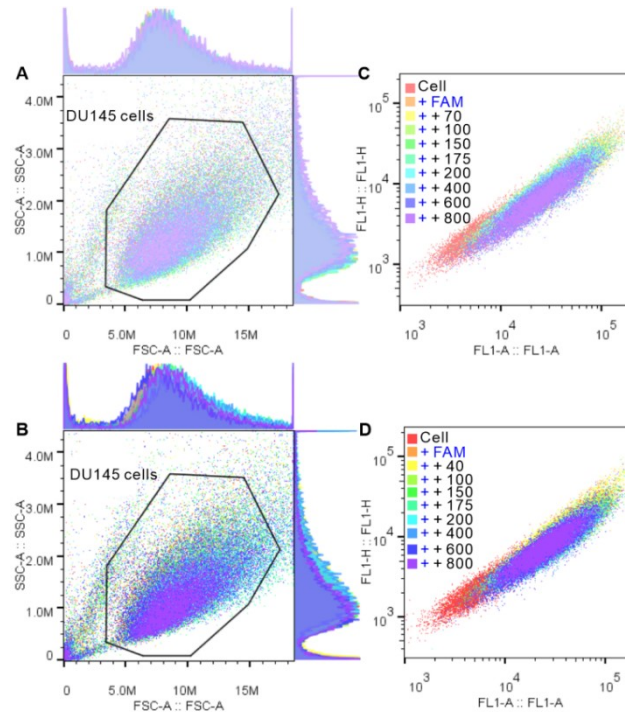


**Figure S20. The population and the monodisperses of the DU145 cells.** (A-D) From up to bottom are native DU145 cells (cell); cells with saturated D7-FAM (+ FAM); cells with saturated D7-FAM and  $G_5@anti\alpha 3(P1B5)$  of different amounts, i.e., 70, 100, 150, 175, 200, 400, 600, and 800  $\mu$ L, respectively (from “+ + 70” to “+ + 800”) in C. From up to bottom are native DU145 cells (cell); cells with saturated DML7-FAM (+ FAM); cells with saturated DML7-FAM and  $G_5@anti\beta 1(K-20)$  of different amounts, i.e., 40, 100, 150, 175, 200, 400, 600, and 800  $\mu$ L, respectively (from “+ + 40” to “+ + 800”).



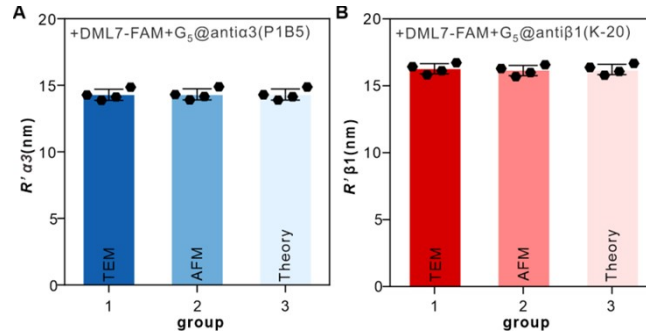


**Figure S21. Statistical analysis exhibited no significant difference among three methods when calculating the separation distance between aptamer binding site and antibody binding site ( $R'$ ).** (A, B) Calculating the  $R'$  between DML7-FAM aptamer and each antibody binding site by three methods, i.e., TEM (group 1), AFM (group 2) and the theoretical calculation (group 3), respectively.  $R'_{\alpha 3}$  and  $R'_{\beta 1}$  represent the separation distance between aptamer binding site and each antibody binding site, i.e., anti $\alpha 3$ (P1B5) and anti $\beta 1$ (K-20), respectively.

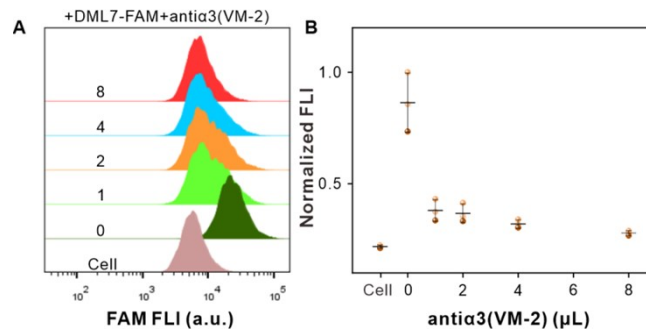


**Figure S22. Competitive binding of another antibody (anti $\alpha 3$ (VM-2)) and DML7-FAM aptamer on integrin protein of DU145 cell membrane.** (A, B) Competitive binding assays between saturated DML7-FAM and different amounts of anti $\alpha 3$ (VM-2) including 1, 2, 4, and 8  $\mu$ L, respectively. The order incubated with cells is DML7-FAM, then antibody.



**Supplemental table****Table S1. The sequence of DNA used in this paper.**

Name	Sequence (5'-3')
XQ-2d-FAM	FAM-C <sub>6</sub> -ACTCATAGGGTTAGGGGCTGCTGGCCAGATA CTCAGATGTAGGGTTACTATGAGC
XQ-2d-1TA-FAM	FAM-C <sub>6</sub> -TACTCATAGGGTTAGGGGCTGCTGGCCAGAT ACTCAGATGGTAGGGTTACTATGAGCA
XQ-2d-2TA-FAM	FAM-C <sub>6</sub> -TTACTCATAGGGTTAGGGGCTGCTGGCCAGA TACTCAGATGGTAGGGTTACTATGAGCAA
XQ-2d-3TA-FAM	FAM-C <sub>6</sub> -TTTACTCATAGGGTTAGGGGCTGCTGGCCAG ATACTCAGATGGTAGGGTTACTATGAGCAAA
XQ-2d-Alexa488	Alexa488-C <sub>6</sub> -ACTCATAGGGTTAGGGGCTGCTGGCCAGA TACTCAGATGTAGGGTTACTATGAGC
XQ-2d-1TA- Alexa488	Alexa488-C <sub>6</sub> -TACTCATAGGGTTAGGGGCTGCTGGCCAG ATACTCAGATGGTAGGGTTACTATGAGCA
XQ-2d-2TA- Alexa488	Alexa488-C <sub>6</sub> -TTACTCATAGGGTTAGGGGCTGCTGGCCA GATACTCAGATGGTAGGGTTACTATGAGCAA
XQ-2d-3TA- Alexa488	Alexa488-C <sub>6</sub> -TTTACTCATAGGGTTAGGGGCTGCTGGCC AGATACTCAGATGGTAGGGTTACTATGAGCAAA
DML7-FAM	FAM-C <sub>6</sub> -ACGCTCGGATGCCACTACAGGTTGGGGTCGG GCATGCGTCCGGAGAAGGGCAAACGAGAGGTCACCA GCACGTCCATGAG

FAM or Alexa488-labeled XQ-2d and FAM-labeled DML7 aptamers were purchased from Sangon Biotech Co., Ltd. (China, Shanghai).

## Supplemental References

1. Hayat, M. A., Colloidal Gold Principles, Methods, and Applications. *Academic Press Inc.* 1989.
2. Yao, L.; Ye, Y.; Teng, J.; Xue, F.; Pan, D.; Li, B.; Chen, W., In Vitro Isothermal Nucleic Acid Amplification Assisted Surface-Enhanced Raman Spectroscopic for Ultrasensitive Detection of *Vibrio parahaemolyticus*. *Anal. Chem.* 2017, *89* (18), 9775-9780.
3. Zhang, L.; Mazouzi, Y.; Salmain, M.; Liedberg, B.; Boujday, S., Antibody-Gold Nanoparticle Bioconjugates for Biosensors: Synthesis, Characterization and Selected Applications. *Biosens. Bioelectron.* 2020, *165*, 112370.
4. Mei, Z.; Deng, Y.; Chu, H.; Xue, F.; Zhong, Y.; Wu, J.; Yang, H.; Wang, Z.; Zheng, L.; Chen, W., Immunochromatographic lateral flow strip for on-site detection of bisphenol A. *Microchimica Acta* 2012, *180* (3-4), 279-285.
5. Song, X.; Zhu, W.; Ge, X.; Li, R.; Li, S.; Chen, X.; Song, J.; Xie, J.; Chen, X.; Yang, H., A New Class of NIR-II Gold Nanocluster-Based Protein Biolabels for In Vivo Tumor-Targeted Imaging. *Angew. Chem. Int. Ed.* 2021, *60* (3), 1306-1312.
6. Younan, N. D.; Sarell, C. J.; Davies, P.; Brown, D. R.; Viles, J. H., The cellular prion protein traps Alzheimer's A $\beta$  in an oligomeric form and disassembles amyloid fibers. *FASEB. J.* 2013, *27* (5), 1847-1858.
7. Zhang, X.; Zhang, L.; Tong, H.; Peng, B.; Rames, M. J.; Zhang, S.; Ren, G., 3D Structural Fluctuation of IgG1 Antibody Revealed by Individual Particle Electron Tomography. *Sci. Rep.* 2015, *5*, 9803.
8. Ouyang, X.; De Stefano, M.; Krissanaprasit, A.; Bank Kodal, A. L.; Bech Rosen, C.; Liu, T.; Helmig, S.; Fan, C.; Gothelf, K. V., Docking of Antibodies into the Cavities of DNA Origami Structures. *Angew. Chem. Int. Ed.* 2017, *56* (46), 14423-14427.